JOURNAL OF VIROLOGY, June 1999, p. 4567–4574 Vol. 73, No. 6
0022-538X/99/$04.00+0

Conformational Intermediates and Fusion Activity of Influenza Virus Hemagglutinin

THOMAS KORTE,[1] KAI LUDWIG,[2] FRANK P. BOOY,[3] ROBERT BLUMENTHAL,[1]* AND ANDREAS HERRMANN[2]*

Laboratory of Experimental and Computational Biology, National Cancer Institute—Frederick Cancer Research & Development Center, National Institutes of Health, Frederick, Maryland 21702[1]; Mathematisch-Naturwissenschaftliche Fakultät I, Institut für Biologie/Biophysik, Humboldt-Universität zu Berlin, D-10115 Berlin, Germany[2]; and National Institute of Arthritis and Musculoskeletal and Skin Disease, National Institutes of Health, Bethesda, Maryland 20892[3]

Received 6 January 1999/Accepted 24 February 1999

Three strains of influenza virus (H1, H2, and H3) exhibited similar characteristics in the ability of their hemagglutinin (HA) to induce membrane fusion, but the HAs differed in their susceptibility to inactivation. The extent of inactivation depended on the pH of preincubation and was lowest for A/Japan (H2 subtype), in agreement with previous studies (A. Puri, F. Booy, R. W. Doms, J. M. White, and R. Blumenthal, J. Virol. 64:3824–3832, 1990). While significant inactivation of X31 (H3 subtype) was observed at 37°C at pH values corresponding to the maximum of fusion (about pH 5.0), no inactivation was seen at preincubation pH values 0.2 to 0.4 pH units higher. Surprisingly, low-pH preincubation under those conditions enhanced the fusion rates and extents of A/Japan as well as those of X31. For A/PR 8/34 (H1 subtype), neither a shift of the pH (to >5.0) nor a decrease of the temperature to 20°C was sufficient to prevent inactivation. We provide evidence that the activated HA is a conformational intermediate distinct from the native structure and from the final structure associated with the conformational change of HA, which is implicated by the high-resolution structure of the soluble trimeric fragment TBHA2 (P. A. Bullough, F. M. Hughson, J. J. Skehel, and D. C. Wiley, Nature 371:37–43, 1994).

The fusion of influenza viruses with target membranes is mediated by the major spike membrane glycoprotein of influenza virus, the hemagglutinin (HA). HA is organized in the viral membrane as a homotrimer; each monomer consists of two disulfide-linked subunits, HA1 and HA2. The HA-mediated fusion is triggered by acidic pH, converting the HA into a fusiogenic conformation. During the past few years, we have probed the conformational landscape which viral envelope glycoproteins navigate when triggered to promote fusion (27). X-ray crystallographic studies of the neutral HA of influenza virus (37) and of fragments of HA2 (9), the transmembrane (TM) subunit of Moloney murine leukemia virus (16), and the gp41 core from human immunodeficiency virus type 1 (HIV-1) (11, 35) provide well-defined landmarks in this terrain. Such studies have led to the proposal that there are native (nonfusiogenic) and fusion-active (fusiogenic) states of viral membrane fusion proteins. Our conformational exploration has unveiled a number of states en route between the native and fusiogenic states, some of which transform into an inactivated state. Interestingly, the conformational transitions are irreversible in influenza virus HA and reversible in vesicular stomatitis virus G (26). Our aim is to examine these conformations in detail and to relate them to the fusion-active states of influenza virus HA.

* Corresponding author. Mailing address for A. Herrmann: Mathematisch-Naturwissenschaftliche Fakultät I, Institut für Biologie/Biophysik, Humboldt-Universität zu Berlin, Invalidenstr. 43, D-10115 Berlin, Germany. Phone: 49-30-20938860. Fax: 49-30-20938585. E-mail: Andreas=Herrmann@rz.hu-berlin.de. Mailing address for R. Blumenthal: Laboratory of Experimental and Computational Biology, National Cancer Institute-FCRDC, National Institutes of Health, Bldg. 469, Rm. 211, Frederick, MD 21702. Phone: (301) 846-5068. Fax: (301) 846-6192. E-mail: blumen@helix.nih.gov.

In the present study, we investigated the influence of low-pH preincubation of various influenza virus strains belonging to different HA subtypes (H1 [A/PR 8/34], H2 [A/Japan/305/57], and H3 [X31]) on the fusion activity of the viruses. Previously, we had shown that at 37°C and pH 5.0, fusion mediated by X31 and A/Japan HA proceeded at similar rates. However, preincubation of the viruses under those conditions in the absence of target membranes resulted in inactivation of X31 HA whereas A/Japan HA remained unaffected (27). We confirmed that the characteristics of the fusion activity and the stability against inactivation processes are typical for each strain. However, preincubation of A/Japan and X31 at suboptimal pH values and 37°C did not lead to inactivation but resulted in the formation of a conformational intermediate in the fusion cascade.

MATERIALS AND METHODS

Materials. Octadecylrhodamine B chloride (R_{18}) and 1,1′-bis(4-anilino)naphthalene-5,5′-disulfonic acid (bis-ANS) were purchased from Molecular Probes (Eugene, Oreg.). Fresh blood from healthy donors was obtained from the Blood Bank, Berlin-Lichtenberg, Germany, and used within 3 days after sampling. Purified influenza virus X31, A/PR/8/34, and A/Japan (A/Japan/305/57) were prepared as described previously (25, 27).

Buffers. The following buffers were used, depending on the desired pH: (i) phosphate-buffered saline (PBS) (5.8 mmol of phosphate per liter, 145 mmol of NaCl per liter; pH 7.4) or (ii) sodium acetate buffer (20 mmol of sodium acetate per liter, 130 mmol of NaCl per liter; pH < 6.0).

Erythrocyte and ghost preparations. After removal of buffy coat and plasma, erythrocytes were washed three times in PBS (pH 7.4). Unsealed erythrocyte ghosts were prepared by the method of Dodge et al. (13).

Purification of HA. The viral membrane was solubilized in 1.5% octylglycoside (Boehringer GmbH, Mannheim, Germany) for 1 h at 4°C. The insoluble material was removed by centrifugation at 100,000 × *g* for 60 min. For purification by affinity chromatography by the method of Doms et al. (14), the supernatant containing the HA in detergent micelles was passed over a CL4B column loaded with ricin A (Sigma Chemical Co., St. Louis, Mo.). HA was eluted with PBS containing 1% galactose in the presence of 1.5% octylglycoside, and the detergent and galactose were removed by dialysis against PBS for about 14 h with one

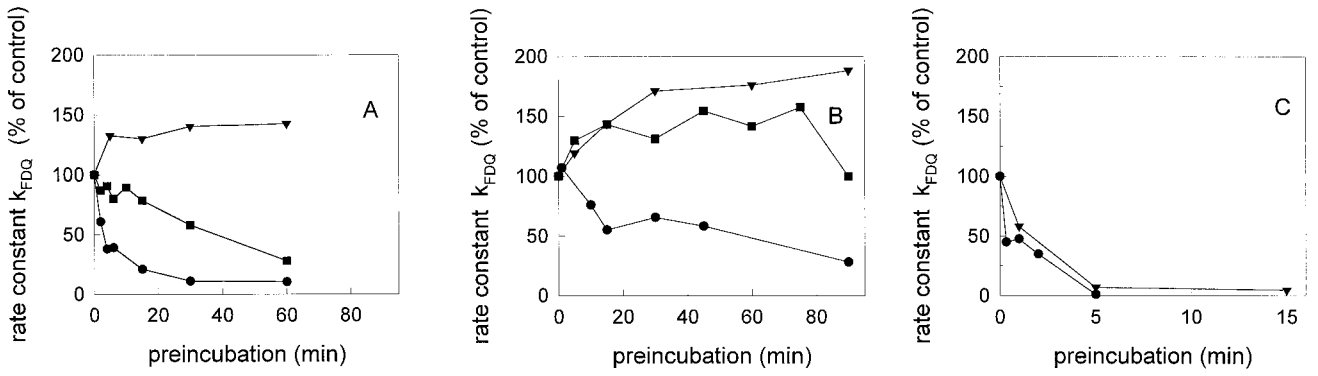

FIG. 1. Influence of low-pH preincubation on the rate constant of influenza virus-ghost fusion at pH 5.0 and 37°C in sodium acetate buffer. (A) influenza virus X31; (B) A/Japan/305/57; (C) A/PR 8/34. Preincubation of R_{18}-labeled influenza virus was done at low pH (●, pH 5.0; ■, pH 5.2; ▼, pH 5.4) and 37°C in the absence of target membranes for the indicated times. Subsequently, the virus sample was reneutralized (pH 7.4) and binding to ghost membranes was performed on ice for 30 min as described in the text. After binding, the fusion was measured at pH 5.0 and 37°C by fluorescence dequenching of R_{18}. To compare the results between the various strains, we have normalized the rate constants to that of the control (set at 100%), which corresponds to the fusion at pH 5.0 and 37°C without any preincubation of viruses at low pH. Fluorescence was measured at excitation and emission wavelengths of 560 and 590 nm, respectively (time resolution, 0.5 s). Note the different scaling of the preincubation times.

buffer change. The purity of the HA was checked by sodium dodecyl sulfate-polyacrylamide gel electrophoresis with 12% gels under reducing conditions (data not shown).

Labeling of virus for fusion. A 1.25-μl volume of a 2 mM stock solution of R_{18} in ethanol was added by rapid vortexing to 0.25 ml of influenza virus (1 mg of virus protein/ml). After incubation for 30 min at room temperature (in the dark), the virus was washed by high-speed centrifugation (45,000 × *g*) with ice-cold PBS to remove unbound R_{18} and resuspended to a concentration of 1 mg of virus protein/ml (2, 17). The final concentration of added probe corresponds to approximately 2 mol% of total viral lipid. The protein concentration of viruses as well as of ghosts was determined by the method of Lowry et al. (23).

Inactivation of influenza virus. Influenza virus (1 mg/ml) was preincubated at low pH (see the figure legends) in the absence of the target membrane. After different periods, samples of the virus suspension were neutralized (pH 7.4) and kept on ice. Subsequently, virus was bound to cell membranes and fusion was measured as described below.

Virus binding to cell membranes. Labeled virus (0.1 mg of protein) was incubated for 30 min on ice with 0.2 ml of erythrocyte ghost suspension (6 to 7 mg of protein/ml). Then the suspension was washed in 10 to 15 volumes of ice-cold PBS and resuspended by adding PBS to a final concentration of 1 mg of virus protein/ml.

Fusion assay. Fusion was measured by monitoring the fluorescence dequenching (FDQ) of the lipid-like fluorophore R_{18} upon fusion of R_{18}-labeled viruses with ghost membranes (18). Fusion was triggered by transferring 30 μl of ice-cold virus-ghost suspension to a quartz cuvette containing 1.8 ml of sodium acetate or PBS buffer at the preadjusted temperature and the respective pH (pH 4.5 to 7.4). The suspension was stirred continuously with a 2- by 8-mm Teflon-coated magnetic stir bar. Fusion was monitored continuously by measuring FDQ (λ_{ex} = 560 nm; λ_{em} = 590 nm; cutoff filter, 570 nm), with a time resolution of 0.5 s, with an AMINCO Bowman II or SHIMADZU RF5001 PC fluorescence spectrometer. At the end of each experiment, Triton X-100 (final concentration, 0.5%) was added to obtain maximum R_{18} fluorescence, F(max). The percentage of FDQ was calculated as described previously (5):

$$\mathrm{FDQ} = 100\% \times \frac{F(t) - F(0)}{F(\mathrm{max}) - F(0)}$$

where $F(0)$ and $F(t)$ are the fluorescence intensity before starting fusion and the fluorescence intensity at a given time, t, respectively.

Analysis of fusion data. To compare the kinetics of FDQ curves independent of the extent, the apparent rate constant, k_{FDQ}, was calculated by relating the initial rate (IR_{FDQ}) to the maximum extent of FDQ (FDQ_{max}):

$$k_{FDQ} = IR_{FDQ}/FDQ_{max}$$

IR_{FDQ} refers to the maximum of the first derivative of the FDQ curves, obtained by the Savitzky-Golay-algorithm with the TableCurve software of Jandel Scientific:

$$IR_{FDQ} = \text{maximum value of } d(\mathrm{FDQ})/d\,t$$

Binding of bis-ANS to HA. A stock solution of bis-ANS was prepared in methanol. HA (final concentration, 4 μg/ml) was added, at preset temperature and pH (pH 4.5 to 7.4), to 2 ml of buffer containing 3.25 nmol of bis-ANS per ml. The increase of bis-ANS fluorescence in the presence of influenza virus was measured at λ_{em} = 490 nm (λ_{ex} = 400 nm). The suspension was stirred continuously with a 2- by 8-mm Teflon-coated magnetic stir bar.

Analysis of bis-ANS data. From plots of the measured bis-ANS fluorescence intensity (I) against time (t), a relative fluorescence, I_{rel}, was calculated

$$I_{rel}(t) = \frac{I(t) - I(0)}{I(\mathrm{pH\ 7.4,\ max}) - I(0)} \quad (1)$$

where $I(0)$ is the fluorescence intensity of bis-ANS in aqueous solution and I(pH 7.4, max) is the final extent of the bis-ANS fluorescence in the presence of the virus at pH 7.4.

Cryoelectron microscopy. The morphology of the intact influenza virus in the native and fusiogenic states was studied by cryoelectron microscopy. Virus samples (2 mg/ml in PBS) preincubated at 37°C for 1 h at the desired pH were applied to a carbon-coated or holey carbon grid and quench-frozen in liquid ethane in a KF80 freezing machine (Reichert, Vienna, Austria). The grid was subsequently transferred to a cooling holder (Gatan Inc., Pleasanton, Calif.) and examined under an EM 400 RT electron microscope (Philips, Eindhoven, Netherlands) under low-dose conditions as described by Booy et al. (8).

RESULTS

Inactivation by preincubation at various pHs. The inactivation of the fusiogenic capacity of various influenza virus strains by low-pH preincubation (in the range from pH 5.4 to 5.0) has been investigated with human erythrocyte ghost membranes as a target. Three different subtypes were chosen: A/PR 8/34 (subtype H1), A/Japan/305/57 (H2), and X31 (H3). HA-mediated fusion was assessed by an FDQ assay with the lipid-like fluorophore R_{18} initially incorporated into the viral membrane. Without low-pH preincubation, all three viruses exhibited a significant fusion activity with erythrocyte membranes at 37°C in the selected pH range from 5.0 to 5.4, as shown previously (21). Both the rate and the extent of fusion were maximum at about pH 5.0. However, for all viruses, even at pH 5.4, significant fusion was observed within the first 10 min upon lowering the pH (21).

To compare the extent of inactivation by preincubation at various pH values, the low-pH pretreated viruses were reneutralized to pH 7.4 and bound to erythrocyte ghosts at 4°C for 30 min. Subsequently, fusion was measured at pH 5.0 and 37°C. We have previously shown that under these conditions there is full fusion of intact virus, i.e., redistribution of lipid, HA, and RNA (24). In Fig. 1, the rate constants of fusion (at pH 5.0 and 37°C) after preincubation of viruses for various times at pH 5.0, 5.2, and 5.4 are shown. The rate constant was deduced from the steepest part of the FDQ kinetics. For comparison of

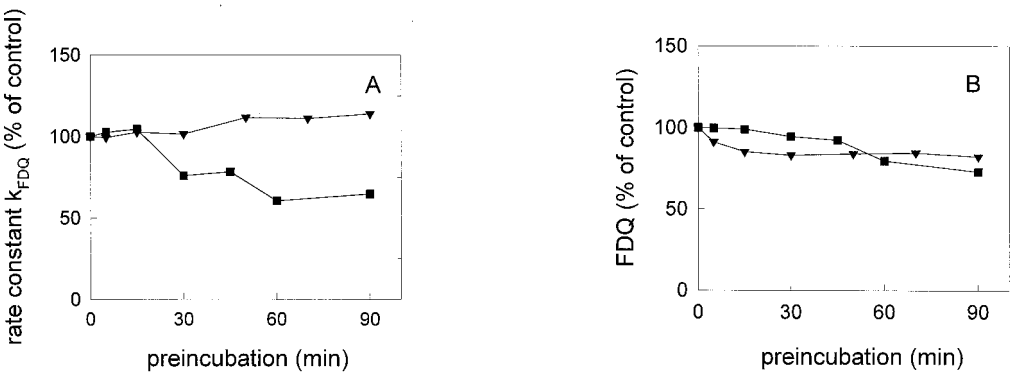

FIG. 2. Influence of preincubation of influenza virus X31 (■) and A/Japan/305/57 (▼) at pH 5.0 and 20°C on the rate constant (A) and extent (B) of virus-ghost fusion at pH 5.0 and 37°C in sodium acetate buffer. Preincubation of influenza virus was done at pH 5.0 and 20°C in the absence of target membranes for the indicated times. Subsequently, the virus sample was reneutralized (pH 7.4) and binding to ghost membranes was performed on ice as described in the text. After binding, the fusion was measured at pH 5.0 and 37°C. To compare the results between the various strains, we have normalized the data to the control (set at 100%), which corresponds to the fusion at pH 5.0 and 37°C without any preincubation of viruses at low pH.

the results among the various strains, we have normalized the data to the respective control (set at 100%), which corresponds to the fusion at pH 5.0 and 37°C without any preincubation of viruses at low pH.

As shown in Fig. 1, the influence of a low-pH preincubation of influenza viruses depended significantly on the virus strain as well as the chosen pH. At pH 5.0, where the most rapid and extensive fusion was observed (21), the fusiogenic activity of X31 disappeared very rapidly. Within 10 min of preincubation at pH 5.0, the rate constant of fusion decreased by more than 70% (Fig. 1A). In contrast to X31, inactivation of A/Japan at pH 5.0 proceeded rather slowly (Fig. 1B), in agreement with the previous results of Puri et al. (27).

For both X31 and A/Japan, low-pH inactivation was significantly reduced or even abolished when preincubation took place at slightly higher pH values (Fig. 1A and B). The rate constant, k_{FDQ}, of X31 declined much more slowly after preincubation at pH 5.2 (Fig. 1A). Remarkably, after preincubation of A/Japan and X31, respectively, at pH 5.4, we observed an enhancement of the rate constant. This was found for A/Japan even after a short preincubation at pH 5.2 (Fig. 1B).

A similar influence of the pH of preincubation was measured for the extent of fusion (21). For X31, a rapid decline of the extent of fusion by about 70% was observed within a 10-min preincubation at pH 5.0 and 37°C. A/Japan became inactivated only slowly under those conditions; after 45 min of preincubation, the extent decreased by about 50%. When the pH of preincubation was shifted to higher values, it became evident again that inactivation was abolished. A preincubation for 90 min at pH 5.4 and 37°C did not affect the extent of fusion of X31. Prolonged preincubation of A/Japan at pH 5.4 and 37°C caused an increase of the extent of fusion by 20 to 40% with respect to the control (no preincubation).

For A/PR 8/34, inactivation was very rapid even after preincubation at pH 5.4. Within 5 min, the fusion activity was almost completely lost, as deduced from the constant k_{FDQ} (Fig. 1C) as well as from the extent of fusion (21).

Temperature dependence of low-pH inactivation. The low-pH inactivation of both X31 and A/Japan was significantly reduced when preincubation at pH 5.0 was performed at lower temperatures. The decline in the rate constant of fusion and of the extent of fusion (Fig. 2) was significantly decelerated after preincubation at 20°C and pH 5.0. The rate constant of A/Japan remained even unaffected. In contrast, for A/PR 8/34, we still observed a fast abolition of the fusion activity by preincubation at 20°C (Fig. 3). Only after lowering the temperature of preincubation to about 3°C did we find a significant reduction of inactivation processes.

Binding of bis-ANS to influenza virus. Hydrophobic interactions between viral fusion proteins and the target membrane seem to be essential for the initiation of the fusion event. We have shown that structural alterations of the HA ectodomain resulting in an exposure of hydrophobic sequences could be monitored continuously by means of the hydrophobicity-sensitive dye bis-ANS (20). The water-soluble fluorophore bis-ANS expresses a significant enhancement of the quantum efficiency upon binding to hydrophobic sites, e.g., those of proteins. We found a strong increase of the fluorescence of bis-ANS in the presence of influenza virus A/PR 8/34 at low pH, which in its pH dependence was very similar to that of the viral fusion activity. An increase in the fluorescence of bis-ANS at low pH was not seen upon enzymatic removal of the ectodomain of HA (20) or for viruses with uncleaved HA (HA0) (21a). Our data indicated that in addition to the hydrophobic N terminus of HA2, other hydrophobic sequences of the ectodomain became accessible to bis-ANS. On the other hand, low-pH-induced inactivation of influenza virus has been associated with an aggregation of several HA trimers, which presumably might be determined by hydrophobic interactions. To elucidate whether the hydrophobic properties of HA are also related to the virus strain-specific inactivation of fusiogenic properties, we have investigated the pH dependence of the bis-ANS fluorescence in the presence of rosettes of isolated HA for the three strains.

In Fig. 4A, the kinetics of the bis-ANS fluorescence in the presence of HA from A/PR 8/34 at various pH values is shown (data not shown for X31 and A/Japan). At time zero, HA was added to prewarmed buffer (37°C) of the desired pH. The fluorescence intensity was related to the maximum extent of the control at pH 7.4 (I_{rel}). A rapid increase of the bis-ANS fluorescence occurred at acidic pH. Association of bis-ANS with HA caused a strong blue shift of the fluorescence spectrum. The wavelength of the fluorescence maximum was shifted from 510 nm (water) to about 485 nm in the presence of HA (data not shown). In Fig. 4B, the final extent of bis-ANS fluorescence in the presence of HA is presented for the three virus strains. The experiments were done at the same HA concentration. The pH dependence of the extent of the bis-ANS fluorescence coincided with that of the fusion activity (Fig. 4C).

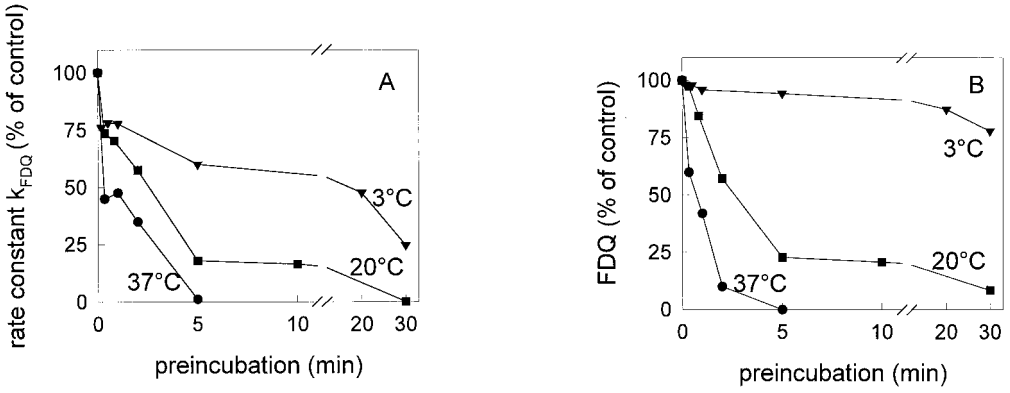

FIG. 3. Influence of temperature on the low-pH inactivation of influenza virus A/PR 8/34 and on the rate constant (A) and extent (B) of virus-ghost fusion at pH 5.0 and 37°C in sodium acetate buffer. Preincubation of influenza virus was done at pH 5.0 and 3°C (▼), 20°C (■), and 37°C (●) in the absence of target membranes for the indicated times. Subsequently, the virus sample was reneutralized (pH 7.4) and binding to ghost membranes was performed on ice as described in the text. After binding, the fusion was measured at pH 5.0 and 37°C. To compare the results between the various strains, we have normalized the data to the control (set at 100%), which corresponds to the fusion at pH 5.0 and 37°C without any preincubation of viruses at low pH.

For the three strains, the pH dependence of the extent of the bis-ANS fluorescence was very similar for intact viruses and rosettes of isolated HA, as shown for A/PR 8/34 (inset in Fig. 4B). Quantitative differences in I_{rel} between isolated HA and intact viruses arise mainly because binding of bis-ANS to the lipid phase of the viral membrane contributes significantly to the fluorescence intensity at pH 7.4 (20). Thus, for intact viruses, the HA-associated fluorescence of bis-ANS at low pH is underestimated by I_{rel} with respect to isolated HA. We cannot preclude the possibility that those differences of I_{rel} also evolve, at least partly, from the tighter packing of HA in viruses. Due to this packing, the number of bindings for bis-ANS becomes limited by the rapid hydrophobic interaction of neighboring HAs upon lowering the pH. Therefore, and to ensure identical HA concentrations for comparison among various influenza strains, the fluorescence of bis-ANS was measured for isolated HA.

At pH 5.0, the extent of the bis-ANS fluorescence occurred in the order X31 > A/PR 8/34 > A/Japan. While a sharp decline of the fluorescence intensity was observed at pH > 5.0 for X31, the intensity decreased more smoothly for A/PR 8/34. Thus, e.g., at pH 5.4, the bis-ANS fluorescence of HA from A/PR 8/34 was twice as much as that of HA from either of the two other strains.

The temperature dependence of the bis-ANS fluorescence in the presence of isolated HA at pH 5.0 is shown for the various virus strains in Fig. 5. At all temperatures, the fluorescence intensity was lowest for A/Japan. A sharp drop of the fluorescence intensity was observed for X31 between 37 and 20°C, while the decline was more gradual for A/PR 8/34. Indeed, even at 10°C a rather high fluorescence emission of bis-ANS (twice as high as that for A/Japan and X31) was detected in the presence of HA from A/PR 8/34.

We have investigated whether the increase in fluorescence of bis-ANS in the presence of HA (A/Japan) was reversible after reneutralization to pH 7.4. We found that the degree of reversibility depended on the pH as well as on the time of preincubation at that pH (Fig. 6). The increase in fluorescence at pH 5.4 was almost completely reversible even after prolonged preincubation. A slow, continuous loss of the reversibility of bis-ANS fluorescence was monitored when HA of A/Japan was preincubated at pH 5.2. However, at pH 5.0, a

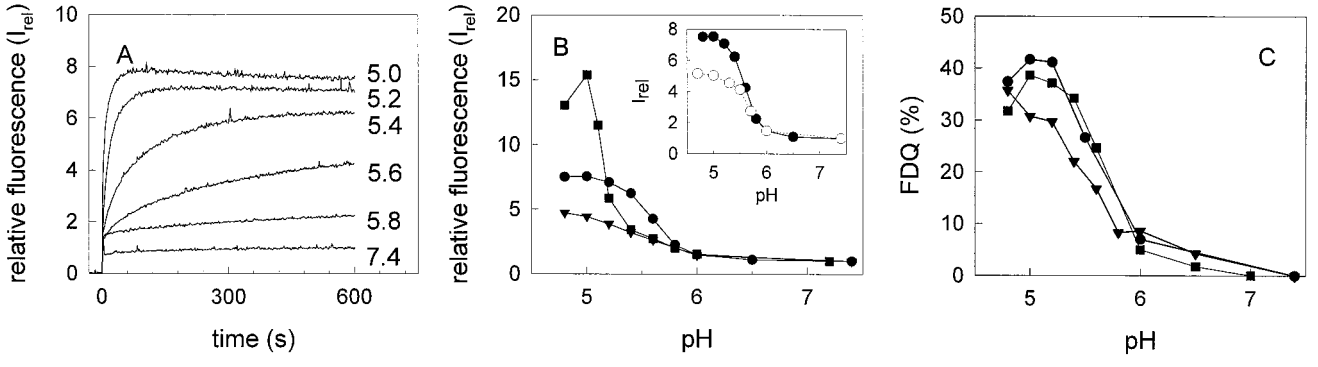

FIG. 4. pH dependence of the bis-ANS fluorescence in the presence of isolated HA and of the extent of virus-ghost fusion of influenza viruses of different subtypes (37°C). (A) Kinetics of the bis-ANS fluorescence in the presence of HA of A/PR 8/34 (data not shown for X31 and A/Japan/305/57). At time zero, HA (4 μg/ml) was added to buffer (37°C) containing 3.25 nmol of bis-ANS per ml. Fluorescence was measured at excitation and emission wavelengths of 400 and 490 nm, respectively (time resolution, 0.5 s). The relative fluorescence, I_{rel}, is shown (see Materials and Methods). (B) Maximum of the relative fluorescence, I_{rel}, of bis-ANS after 10 min of incubation at the desired pH. (C) Virus-ghost fusion. Fusion was measured at the indicated pH and 37°C for 20 min by the FDQ assay with the lipid-like fluorophore R_{18} (see the legend to Fig. 1). ▼, A/Japan/305/57; ■, X31; ●, A/PR 8/34. (Inset to panel B) Comparison of bis-ANS fluorescence in the presence of isolated HA of A/PR 8/34 (●) or intact A/PR 8/34 (○). Bis-ANS fluorescence in the presence of intact viruses (20 μg of virus protein/ml) was measured as described for isolated HA.

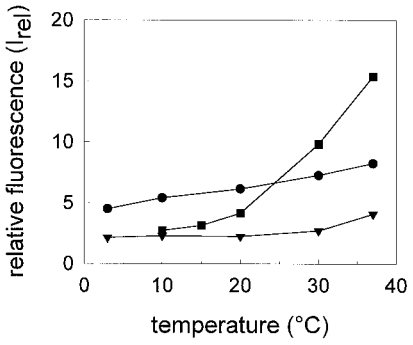

FIG. 5. Temperature dependence of the bis-ANS fluorescence, I_{norm}, at pH 5.0 in the presence of HA (4 μg/ml) of different influenza virus subtypes. ▼, A/Japan/305/57; ■, X31; ●, A/PR 8/34. The maximum of the relative fluorescence, I_{rel}, of bis-ANS (3.25 nmol/ml) after 10 min of incubation at pH 5.0 at the desired temperature is shown. For details, see the legend to Fig. 4 and Materials and Methods.

significant amount of the bis-ANS fluorescence became rapidly irreversible.

DISCUSSION

The three subtypes of influenza virus HA considered in the present study exhibited similar characteristics in their ability to induce membrane fusion but differed in their susceptibility to inactivation. The extent of inactivation was lowest for A/Japan (H2 subtype), in agreement with previous results (27), and depended on the pH of preincubation. While significant inactivation of X31 and A/Japan was observed at 37°C at pH values corresponding to the fusion maximum (about pH 5.0), no inactivation was seen at a pH of preincubation that was 0.2 to 0.4 unit higher. Surprisingly, low-pH preincubation under those conditions enhanced the fusiogenic properties of HA, resulting in an increase of the rate and extent of fusion for A/Japan as well as for X31. For A/PR 8/34, neither a shift of the pH (to >5.0) nor a decrease of the temperature (to 20°C) was sufficient to prevent inactivation.

Recently, we compared the conformational changes undergone by HA of X31 and A/Japan following exposure to pH 5 and 37°C for 15 min (27). Under these conditions, there was no change in spike morphology of the A/Japan HA, whereas X31

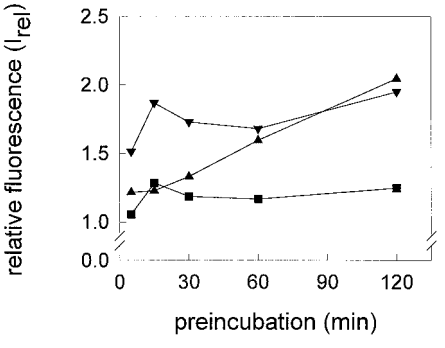

FIG. 6. Reversibility of the low-pH fluorescence of bis-ANS in the presence of HA of A/Japan/305/57 (4 μg/ml). After preincubation of HA at pH 5.0 (▼), pH 5.2 (▲), or pH 5.4 (■), the fluorescence was measured at pH 7.4 for 15 min. The relative fluorescence, I_{rel}, is presented (see equation 1 in Materials and Methods; $I(t)$ corresponds to the fluorescence intensity after neutralization). All steps were done at 37°C. The concentration of bis-ANS was 3.25 nmol/ml. For details, see the legend to Fig. 4 and Materials and Methods.

HA showed a fuzzy appearance. However, the pH 5- and 37°C-treated A/Japan HA had undergone conformational changes as indicated by increased hydrophobicity, exposure of antibody epitopes, and susceptibility to protease digestion. Moreover, the pH 5- and 37°C-treated A/Japan HA was still fusion active, whereas the similarly treated X31 was inactive. Based on these observations, we proposed a three-state model which relates the conformational transitions of HA to mechanisms of viral fusion (6). According to this model, HA undergoes a proton-driven shift from a T (tense) state at neutral pH to a state maintaining the typical spike morphology of HA trimers. This metastable state, which is relaxed with respect to the T state, was termed R. The R state was followed by a transition to the D (desensitized) state, for which the fuzzy morphology is characteristic. We suggested that the conformation of the pH 5- and 37°C-treated A/Japan HA corresponded to the R state while that of the pH 5- and 37°C-treated X31 HA corresponded to the D state.

Our observation in this study revealed that pH 5.4- and 37°C-treated X31 HA is not inactivated but is even more fusion active. This indicates that it might be in the R state. Figure 7 shows cryoelectron microscopy images of X31 treated at 37°C and pH 7.4, pH 5.4, and pH 5.0, respectively. Remarkably, at pH 5.4, the spike morphology observed at pH 7.4 was retained. Only the contours of the spikes seem to be less well defined as those seen at pH 7.4. However, the resolution of these images is not sufficient to characterize this in more detail. This little-changed spike morphology of pH 5.4- and 37°C-treated X31 HA strongly implies that it is in the R state. We note that the small change of the spike morphology is seen over the entire viral membrane, suggesting that all HAs have undergone a transition to the R state. The fuzzy spike morphology of pH 5.0- and 37°C-treated X31 HA supports the notion that it is in the D state. Shangguan et al. (33) recently showed that inactivation of A/PR/8/34 HA at pH 4.9 and 30°C correlated with loss of spike morphology as determined by cryoelectron microscopy, confirming the R and D state assignments we had proposed for the other HA strains.

Previously we had monitored continuously the transient stages of the HA tertiary structure at acidic pH by time-resolved circular dichroism (CD) spectroscopy in the near UV (21). After acidification, initially a fusion-competent intermediate of HA was formed which is characterized by a rearrangement but not a loss of the tertiary structure. Subsequently, we observed a continuous loss of the tertiary structure. The fusion-competent state was kinetically stabilized by suboptimal pH (pH 5.4) or lower temperatures (20°C). These two states can be assigned to the R and D states, respectively, consistent with the cryoelectron microscopy images. Although our CD measurement showed that formation of the R state is accompanied by alterations in the tertiary structure, they do not provide clear evidence that all HAs have undergone a transition. However, differential scanning calorimetry of HA indicates that all the HAs undergo a thermal transition at a given pH with a characteristic transition temperature T_m and enthalpy H_{cal}. At pH 7.4, 5.4 and 5.0 these are 66.5°C and 980 kcal/mol, 45.1°C and 204 kcal/mol, and 41.8°C and 73 kcal/mol, respectively (22a). The sharpness of the transitions indicates that at a given pH, all HAs assume a given conformation, consistent with our conclusion from cryoelectron microscopy (see above).

We found a correlation between the hydrophobic properties of HA deduced from the binding of bis-ANS and the inactivation of influenza virus. Inactivation of A/Japan HA by preincubation at pH 5.0 proceeded more slowly than that of X31 and A/PR 8/34 HA. Likewise, the hydrophobicity of A/Japan

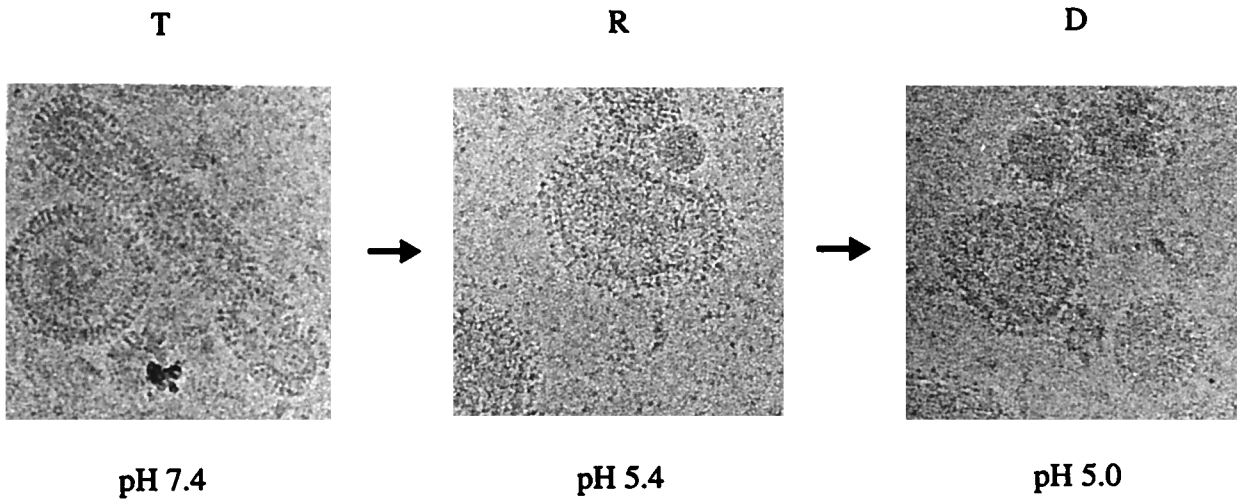

FIG. 7. Cryoelectron micrographs of whole influenza virus X31 (2 mg/ml) after incubation at 37°C and pH 7.4 (A), pH 5.3 (B), and pH 4.9 (C).

HA was lower than that of X31 and A/PR 8/34 at pH 5.0. After preincubation at pH 5.4, we observed no inactivation of X31 and A/Japan HA but we observed a rapid loss of the fusiogenic activity of A/PR 8/34. This coincides with a significantly higher hydrophobicity of HA of A/PR 8/34 than of the other virus strains. The correlation between the exposure of hydrophobicity of HA and inactivation is sustained by the temperature dependence of both processes. We found that inactivation at 20°C by preincubation at pH 5.0 was very slow for X31 and A/Japan but rapid for A/PR 8/34. As shown by the binding of bis-ANS to HA, the hydrophobicity of HA of A/PR 8/34 was much higher than that of HA of X31 and A/Japan. Only at rather low temperature (3°C) was inactivation of A/PR 8/34 by preincubation at pH 5.0 significantly diminished. However, it was still faster than that observed for X31 and A/Japan at 20°C. These results point to a correlation between the inactivation and hydrophobicity of HA at low pH. However, hydrophobic properties of HA are not the sole determinant of inactivation. This becomes evident from the data at pH 5.0 and 37°C. Although bis-ANS fluorescence indicates a higher hydrophobicity of HA from X31 than of that from A/PR 8/34, inactivation of the latter strain was faster than that of X31. Presumably more hydrophobic sites are exposed under these conditions in X31 when the HA molecules fall apart. However, under suboptimal conditions for inactivation of X31 (pH 5.4 and 37°C or pH 5 and 20°C), A/PR 8/34 is inactivated. Under those conditions we found the following for bis-ANS: A/PR 8/34 > X31 = A/Japan (pH 5.4 and 37°C [Fig. 4B]) and A/PR 8/34 > X31 > A/Japan (pH 5.0 and 20°C [Fig. 5]).

Is the exposure of hydrophobic sites of HA a result or a determinant of the inactivation of the fusiogenic activity and the loss of tertiary structure of influenza virus HA? Our data on the reversibility of bis-ANS binding to HA of A/Japan at low pH upon reneutralization support the latter view. We found that at pH 5.2 the binding was initially almost reversible. Although the fluorescence and thus the extent of binding of bis-ANS to HA did not increase further (Fig. 6), the bis-ANS fluorescence became irreversible only after prolonged incubation. A similar time dependence was observed for the inactivation of the fusiogenic capacity of A/Japan by preincubation at pH 5.2. Only after prolonged preincubation did we find a decrease of the fusiogenic activity of this virus. The fusion peptide sequence of HA (15) is a good candidate for the initial appearance of hydrophobic sites associated with fusion activity (34, 36). We have previously shown that the interaction of bis-ANS with the fusion sequence becomes intensified at acidic pH. The subsequent enhanced bis-ANS fluorescence associated with inactivation is caused by the exposure of additional hydrophobic sites (10, 20), presumably in the interfaces following the dissociation of HA1-HA2 trimers in the D state, consistent with the cryoelectron microscopy images (27). Such a sequential conformational change is in accordance with the observation of White and Wilson (36), who measured the kinetics of the conformational change of strain X31 HA by using a set of antibodies. They proposed a model which assumes that the low-pH-mediated conformational change occurs in two major steps. In the first step the fusion peptide becomes exposed, which is fast even under suboptimal conditions. In the second step the globular heads of the trimers dissociate and open. The half time of the latter step is very sensitive to temperature and pH.

In previous studies on the kinetics of influenza virus HA-mediated fusion, we focused on events which occurred after the conformational change (5, 7). Those studies revealed a number of intermediates in the fusion cascade, including formation of a transient fusion pore, a hemifusion diaphragm which allows lipid redistribution, and a large pore which allows transfer of solutes. In the present study, we have examined conformational intermediates. Previous studies on the kinetics of low-pH-triggered conformational changes of isolated X31 HA rosettes (21, 22) indicated very rapid changes at pH 5 and 37°C. The fact that we observed a conformational intermediate in this study indicates that these changes might be slower (even rate limiting) in the intact virus bound to the target membrane. The argument is as follows. If HA in the T state becomes bound to the membrane (T_M) the reaction scheme goes according to $T_M \rightarrow R_M \rightarrow F$ (scheme 1), where R_M is HA in the R state bound to the membrane and F is the fusion pore. If HA is first brought to the R state and then bound to the membrane (R_M), the reaction scheme goes according to $R_M \rightarrow F$ (scheme 2). If the rate of fusion according to scheme 1 is equal to that according to scheme 2, the $T_M \rightarrow R_M$ transition is rapid. However, for X31 and A/Japan HA, we find conditions where the rate of fusion according to scheme 1 is lower than that according to scheme 2. This indicates that the $T_M \rightarrow R_M$ is rate limiting under these conditions. Thus, R_M represents a con-

formational intermediate which is at least kinetically stable even at neutral pH. Transition of R_M to a conformation which forms a fusion pore requires an acidic pH. Thus, R_M is upstream of the commitment state of HA, which we have previously identified (32). This intermediate is characterized by a stable noncovalent hydrophobic interaction of HA, most probably HA2, with the target membrane. The commitment state can convert to a fusion pore at elevated temperatures (37°C) even at neutral pH. However, the morphology of the commitment state is not known.

We note that we have always measured the fusion of influenza virus at the pH optimal for fusion (pH 5.0). We have previously shown that untreated influenza virus fuses fully to erythrocyte membranes under such conditions (24). This was demonstrated by both HA and RNA redistribution. It remains to be shown that low-pH-pretreated HA trimers also induce full fusion after optimal conditions have been established, since the R_{18} assay does not allow us to discriminate between hemifusion and full fusion. However, we consider it unlikely that lipid mixing is faster with pretreated virus than for untreated virus but that pore dilation is slower or nonexistent.

Can we assign a three-dimensional structure and function to R? Of course, cryoelectron microscopy as applied here does not allow a sufficiently detailed spatial resolution to elucidate the three-dimensional structure of the R state. However, our results show that the kinetically stable R state corresponds to a structure which has retained the spike morphology but bears structural arrangements which are different from the spikes of the T state, i.e., the native cleaved HA as indicated by cryoelectron microscopy, CD, and differential scanning calorimetry measurements (see above). Presumably, R primes HA for the subsequent exposure of the N terminus of HA2 to the target membrane. Based on the X-ray crystal structure of a fragment of the HA ectodomain from X31 in its low-pH form, Bullough et al. (9) suggested that the "fusion sequence" moves toward the top of the ectodomain by the formation of a long α-helix in the HA2 subunit at low pH, thereby extending the trimer stem straight up. We emphasize that the R and D states refer to the whole HA1-HA2 molecule and not to the trimeric coiled-coil fragment (TBHA2), whose crystal structure has been determined and proposed to reflect the fusion-active state (F) (9). If the formation of this structure requires that the HA1 tops fall, the trimeric coiled-coil structure is unlikely to be part of the R state but it might be embedded in the D state, since its fuzzy appearance suggests the dissociation of HA1 tops. However, if the formation of the coiled-coil structure requires only a slight displacement but not a fall of the HA1 tops, an alternative view is that the preservation of spike morphology with the tight association of the monomers, as in R, may ensure the formation of this long α-helix toward the target membrane (29).

We have shown that low-pH-induced conformational changes of HA are not necessarily accompanied by an inactivation process even at 37°C. Although this depends very strongly on the virus strain, the pH is a major factor in separating inactivation from fusion. Thus, with X31 and A/Japan HA, significant fusion can be observed at suboptimal pH values at which no inactivation occurs. This does not contradict a model in which the activation energy needed to drive R into the conformation corresponding to F is the same as that needed to transform it into an inactivated state (3, 30). At suboptimal pH only in the presence (not in the absence) of the closely approached target membrane, the required activation energy is provided to convert R into F. Thus, preincubation of virus in the absence of the target membrane at suboptimal pH does not cause inactivation. Optimal pH (around pH 5.0) is sufficient to trigger $R_M \rightarrow F$. However, in the absence of the target membrane, R transforms irreversibly to the inactivated state. The pH-dependent separation between fusion and inactivation suggests that inactivation in the endosome may not play a significant role for influenza virus. Since it is reasonable to assume that the pH within the endosome lumen is gradually changed, pH conditions at which fusion but not inactivation occurs will transiently exist in the endosome.

Our discovery of a conformational intermediate is not unique for influenza virus HA. Previously we had shown that preexposure of the vesicular stomatitis virus (rhabdovirus) glycoprotein to low pH led to activation of its fusiogenic activity (28). Similar findings were reported on the envelope glycoproteins of HIV-1 and HIV-2 and simian immunodeficiency virus in response to receptor binding by using a soluble form of CD4 (sCD4) as a receptor mimic. We had shown that conformational changes in cell surface HIV-1 envelope glycoproteins which lead to fusion are triggered by cooperation between cell surface CD4 and coreceptors (19). However, binding of sCD4 to the envelope glycoproteins of HIV-1-, HIV-2-, and SIV-infected cells induces certain conformational changes (19, 31). In several cell line-passaged isolates of HIV-1, this interaction leads to inactivation of the virus (31), whereas fusion activity of various HIV-2 and SIV envelope glycoproteins is enhanced by subinhibitory doses of sCD4 (1, 12). The differences in susceptibility to inactivation by sCD4 have been attributed to stabler bonding between envelope glycoprotein subunits in HIV-2 and SIV (31). Similar explanations can be invoked regarding the susceptibility of the different strains of HA to inactivation by low pH. The examination of conformational intermediates may have implications for the development of drugs or vaccines which prevent viral entry. Our result may provide also some input into the determination of the three-dimensional structure of the HA ectodomain at low pH. The R intermediate is less hydrophobic than subsequent states of the conformational change. Thus, the ectodomain in the R state may provide a promising object for crystallization and subsequent X-ray studies.

ACKNOWLEDGMENTS

T.K. is supported by the intramural AIDS targeted antiviral program of the NIH. This work was supported by grant SFB 312 from the Deutsche Forschungsgemeinschaft to A.H.

REFERENCES

1. **Allan, J. S., J. Strauss, and D. W. Buck.** 1990. Enhancement of SIV infection with soluble receptor molecules. Science **247:**1084–1088.
2. **Arbuzova, A., T. Korte, P. Müller, and A. Herrmann.** 1994. On the validity of lipid dequenching assays for estimating virus fusion kinetics. Biochim. Biophys. Acta **1190:**360–366.
3. **Bentz, J.** 1992. Intermediates and kinetics of membrane fusion. Biophys. J. **63:**448–459.
4. **Blumenthal, R., C. Schoch, A. Puri, and M. J. Clague.** 1991. A dissection of steps leading to viral envelope protein-mediated membrane fusion. Ann. N. Y. Acad. Sci. **635:**285–296.
5. **Blumenthal, R., A. Bali-Puri, A. Walter, D. Covell, and O. Eidelman.** 1987. pH-dependent fusion of vesicular stomatitis virus with Vero cells: measurement by dequenching of octadecyl-rhodamine fluorescence. J. Biol. Chem. **262:**13614–13619.
6. **Blumenthal, R., A. Puri, D. P. Sarkar, Y. Chen, O. Eidelman, and S. J. Morris.** 1989. Membrane fusion mediated by viral spike glycoproteins, p. 197–217. *In* A. Helenius, R. Compans, and M. Oldstone (ed.), Cell biology of virus entry, replication and pathogenesis. Alan R. Liss, Inc., New York, N.Y.
7. **Blumenthal, R., D. P. Sarkar, S. Durell, D. E. Howard, and S. J. Morris.** 1996. Dilation of the influenza hemagglutinin fusion pore revealed by the kinetics of individual cell-cell fusion events. J. Cell Biol. **135:**63–71.
8. **Booy, F. P., R. W. Ruigrok, and E. F. van Bruggen.** 1985. Electron microscopy of influenza virus. A comparison of negatively stained and ice-embedded particles. J. Mol. Biol. **184:**667–676.
9. **Bullough, P. A., F. M. Hughson, J. J. Skehel, and D. C. Wiley.** 1994. Structure of influenza haemagglutinin at the pH of membrane fusion. Nature **371:**37–43.

10. **Burger, K. N. J., S. A. Wharton, R. A. Demel, and A. J. Verkleij.** 1991. Interaction of influenza virus hemagglutinin with a lipid monolayer. A comparison of the surface activities of intact virions, isolated hemagglutinins and a synthetic fusion peptide. Biochemistry **30:**11173–11180.
11. **Chan, D. C., D. Fass, J. M. Berger, and P. S. Kim.** 1997. Core structure of gp41 from the HIV envelope glycoprotein. Cell **89:**263–273.
12. **Clapham, P. R., A. McKnight, and R. A. Weiss.** 1992. Human immunodeficiency virus type 2 infection and fusion of CD4-negative human cell lines: induction and enhancement by soluble CD4. J. Virol. **66:**3531–3537.
13. **Dodge, J. T., C. Mitchell, and D. J. Hanahan.** 1963. The preparation and chemical characteristics of hemoglobin free ghosts of human erythrocytes. Arch. Biochem. Biophys. **100:**119–130.
14. **Doms, R. W., A. Helenius, and J. White.** 1985. Membrane fusion activity of the influenza virus hemagglutinin: the low pH-induced conformational change. J. Biol. Chem. **260:**2973–2981.
15. **Durell, S., I. Martin, J. Ruysschaert, Y. Shai, and R. Blumenthal.** 1997. What studies with fusion peptides tell us about viral envelope glycoprotein-mediated membrane fusion. Mol. Membr. Biol. **14:**97–112.
16. **Fass, D., S. C. Harrison, and P. S. Kim.** 1996. Retrovirus envelope domain at 1.7 angstrom resolution. Nat. Struct. Biol. **3:**465–469.
17. **Herrmann, A., M. J. Clague, and R. Blumenthal.** 1993. Enhancement of viral fusion by non-adsorbing polymers. Biophys. J. **65:**528–534.
18. **Hoekstra, D., T. de Boer, K. Klappe, and J. Wilschut.** 1984. Fluorescence method for measuring the kinetics of fusion between biological membranes. Biochemistry **23:**5675–5681.
19. **Jones, P. L., T. Korte, and R. Blumenthal.** 1998. Conformational changes in cell surface HIV-1 envelope glycoproteins are triggered by cooperation between cell surface CD4 and co-receptors. J. Biol. Chem. **273:**404–409.
20. **Korte, T., and A. Herrmann.** 1994. pH-dependent binding of the fluorophore bis-ANS to influenza virus reflects the conformational change of hemagglutinin. Eur. Biophys. J. **23:**105–113.
21. **Korte, T., K. Ludwig, M. Krumbiegel, D. Zirwer, G. Damaschun, and A. Herrmann.** 1997. Transient changes of the conformation of hemagglutinin of influenza virus at low pH detected by time-resolved circular dichroism spectroscopy. J. Biol. Chem. **272:**9764–9770.
21a. **Korte, T., and A. Herrmann.** Unpublished results.
22. **Krumbiegel, M., A. Herrmann, and R. Blumenthal.** 1994. Kinetics of the low-pH-induced conformational changes and fusogenic activity of influenza hemagglutinin. Biophys. J. **67:**2355–2360.
22a. **Krumbiegel, M., D. Remeta, A. Ginsburg, and R. Blumenthal.** Unpublished results.
23. **Lowry, O. H., N. J. Rosebrough, A. L. Farr, and R. J. Randall.** 1951. Protein measurement with the Folin phenol reagent. J. Biol. Chem. **193:**265–275.
24. **Lowy, R. J., D. P. Sarkar, M. H. Whitnall, and R. Blumenthal.** 1995. Differences in dispersion of influenza virus lipids and proteins during fusion. Exp. Cell Res. **216:**411–421.
25. **Pak, C. C., M. Krumbiegel, and R. Blumenthal.** 1994. Intermediates in influenza PR/8 hemagglutinin-induced membrane fusion. J. Gen. Virol. **75:**395–399.
26. **Pak, C. C., A. Puri, and R. Blumenthal.** 1997. Conformational changes and fusion activity of vesicular stomatitis virus glycoprotein: ^{125}iodonaphthylazide photo labeling studies in biological membranes. Biochemistry **36:**8890–8896.
27. **Puri, A., F. Booy, R. W. Doms, J. M. White, and R. Blumenthal.** 1990. Conformational changes and fusion activity of influenza hemagglutinin of the H2 and H3 subtypes: effects of acid pretreatment. J. Virol. **64:**3824–3832.
28. **Puri, A., J. Winick, R. J. Lowy, D. Covell, O. Eidelman, A. Walter, and R. Blumenthal.** 1988. Activation of vesicular stomatitis virus fusion with cells by pretreatment at low pH. J. Biol. Chem. **263:**4749–4753.
29. **Qiao, H., S. L. Pelletier, L. Hoffman, J. Hacker, R. T. Armstrong, and J. M. White.** 1998. Specific single or double proline substitutions in the "spring-loaded" coiled-coil region of the influenza hemagglutinin impair or abolish membrane fusion activity. J. Cell Biol. **141:**1335–1347.
30. **Ramalho-Santos, J., S. Nir, N. Düzgünes, A. Pato de Carvalho, and M. C. Pedroso de Lima.** 1993. A common mechanism for influenza virus fusion activity and inactivation. Biochemistry **32:**2771–2779.
31. **Sattentau, Q. J., J. P. Moore, F. Vignaux, F. Traincard, and P. Poignard.** 1993. Conformational changes induced in the envelope glycoproteins of the human and simian immunodeficiency viruses by soluble receptor binding. J. Virol. **67:**7383–7393.
32. **Schoch, C., R. Blumenthal, and M. Clague.** 1992. A long lived state for influenza virus-erythrocyte complexes committed to fusion at neutral pH. FEBS Lett. **311:**221–225.
33. **Shangguan, T., D. P. Siegel, J. D. Lear, P. H. Axelsen, D. Alford, and J. Bentz.** 1998. Morphological changes and fusogenic activity of influenza virus hemagglutinin. Biophys. J. **74:**54–62.
34. **Stegmann, T., J. M. White, and A. Helenius.** 1990. Intermediates in influenza induced membrane fusion. EMBO J. **9:**4231–4241.
35. **Weissenhorn, W., A. Dessen, S. C. Harrison, J. J. Skehel, and D. C. Wiley.** 1997. Atomic structure of the ectodomain from HIV-1 gp41. Nature **387:**426–428.
36. **White, J. M., and I. A. Wilson.** 1987. Anti-peptide antibodies detect steps in a protein conformational change: low-pH activation of the influenza virus hemagglutinin. J. Cell Biol. **105:**2887–2896.
37. **Wilson, I. A., J. J. Skehel, and D. C. Wiley.** 1981. Structure of the haemagglutinin membrane glycoprotein of influenza virus at 3 A resolution. Nature **289:**366–373.